JOURNAL OF GEOPHYSICAL RESEARCH, VOL. 106, NO. B7, PAGES 13,455–13,472, JULY 10, 2001

Frictional response induced by time-dependent fluctuations of the normal loading

Hugo Perfettini[1] and Jean Schmittbuhl
Laboratoire de Géologie, Ecole Normale Supérieure, Paris, France

James R. Rice
Division of Applied Science and Department of Earth and Planetary Sciences
Harvard University, Cambridge, Massachusetts

Massimo Cocco
Istituto Nazionale di Geofisica, Rome, Italy

Abstract. We study the effect of time-variable normal stress perturbations on a creeping fault which satisfies a velocity-weakening rate- and state-dependent friction law and is slipping at constant speed. We use the spring-block model and include the effect of inertia. To account for the variable normal stress, we use the description introduced by *Linker and Dieterich* [1992], which links normal stress fluctuations to changes of the state variable. We consider periodic perturbations of the normal stress in time (as caused, for instance, by tides) and compare the behavior for two commonly used friction laws (the "slip" and the "ageing" laws). Their mechanical response is shown to be significantly different for normal stress fluctuations. It could be used to probe these two laws during laboratory friction experiments. We show that there is a resonance phenomenon, involving strong amplification of the shear and velocity response of the interface, when the spring stiffness is modestly above its critical value (or when, at a given stiffness, the normal stress is modestly below its critical value). We show that such an amplification is also observed when periodic fluctuations of the shear loading are considered, making the resonance phenomenon a general feature of the response of a near-critical creeping surface to periodic fluctuations of the external loading. Analytical solutions are based on a linear expansion for low amplitude of normal or shear stress variations and are in very good agreement with numerical solutions. A method to find the evolution of friction in the case of an arbitrary perturbation of the normal stress is also presented. The results show that a creeping fault may be destabilized and enter a stick-slip regime owing to small normal stress oscillations. This may also account for a mechanism for the generation of "creep bursts." However, these phenomena require very specific parameter ranges to excite the resonance, which may not be met very generally in nature. This study illustrates the importance of the normal stress fluctuations on stable sliding and suggests further friction laboratory experiments.

1. Introduction

Different approaches have been used to study the instability of frictional sliding between two elastic media using rate- and state-dependent friction laws. Models can be divided into two classes:

The first class consists of discrete models of the spring-block (SB) type, where the elastic medium is modeled as a spring loading a rigid block. The dynamics of this system has been studied for instance by *Rice and Ruina* [1983] and *Rice and Tse* [1986] using rate-and-state friction laws, and quasi-static stability analyses have been carried out by *Ruina* [1983], *Gu et al.* [1984], and *Ranjith and Rice* [1999]. By introducing springs between blocks, the SB system can be extended to an array as in the Burridge-Knopoff model [*Burridge and Knopoff*, 1967; *Carlson and Langer*, 1989; *Schmittbuhl et al.*, 1996].

[1]Now at Laboratoire de Géophysique Interne et Tectonophysique, Université Joseph Fourier, Grenoble, France.

Paper number 2000JB900366.
0148-0227/01/2000JB900366$09.00

The models that consider a continuum elastodynamic description of the elastic medium are more realistic. Examples of such models with rate-and-state laws are given by *Rice and Ruina* [1983], *Okubo* [1989], *Cochard and Madariaga* [1994, 1996], *Rice and Ben-Zion* [1996], and *Ben-Zion and Rice* [1997].

All these works assume constant normal stress on the fault. This assumption is correct if one considers an active fault as a slip discontinuity distributed along an infinite and planar surface surrounded by a homogeneous elastic medium. None of these conditions are verified in nature, making normal stress variations inescapable. Normal stress variations have been considered in a subclass of SB models, by *Dieterich and Linker* [1992] and *He et al.* [1998], by inclining the loading spring with respect to the slipping direction. This inclination of the spring creates a coupling between the shear and the normal stress evolution. Another type of coupling between shear and normal stress has been introduced by *Segall and Rice* [1995] using the SB model; a poroelastic interface induces an evolution of effective normal stress σ via the evolution of the pore pressure P.

For the elastodynamic models, normal stress variations have been considered when the interface subject to friction separates different elastic materials [*Weertman*, 1980; *Adams*, 1995; *Martins and Simões*, 1995; *Andrews and Ben-Zion*, 1997; *Cochard and Rice*, 2000]. In this case interaction between normal and tangential deformation exists (due to a material contrast) so that normal stress is no longer constant and strongly destabilizes the interface response.

Normal stress can also be affected by the change of external loading due to tectonic forces or nearby earthquakes. These latter effects seem to influence seismicity [*Parsons et al.*, 1999] as well as slip of future earthquakes [*Perfettini et al.*, 1999]. Therefore a complete description of the earthquake process should account for variation of normal stress in space as well as in time.

To examine the effect of variable normal stress on a sliding surface, we focus on temporal fluctuations of the normal load. In nature, such variations may be of a transient type, such as seismic waves, or periodic as earth tides or cycling filling or draining of reservoirs. This study concentrates on the later category that are the root of permanent variations of the normal load.

For simplicity, in this first study we use the SB model. This model has provided successful modeling of most laboratory experiments [*Dieterich*, 1979a, 1979b; *Baumerger et al.*, 1995]. The validity of such a framework for modeling frictional behavior of a real fault will be discussed further in section 8. We focus on stable sliding or creep and study the effect of the period of normal or shear stress perturbations on the stability of the fault and the magnitude of this response.

We start with a presentation of the model and focus on implications for friction laboratory experiments. Mainly two laws have been proposed to model the dynamical evolution of frictional strength observed at laboratory scale. They are usually labeled as the Dieterich "ageing" law and the Ruina "slip" law (see section 2). As long as normal stress remains constant, differences between them are difficult to observe. However, when applied to model earthquakes sequences, *Rice and Ben-Zion* [1996] show that the Ruina law shows less complex slip sequences than the Dieterich law, which illustrates the importance to study the range of validity of these two friction laws. When variations of the normal load occur, we show that these two laws can behave significantly differently. On the basis of numerical experiments we suggest laboratory experiments to probe friction laws.

We also examine their common features in response to periodic normal stress variations, since they become identical when linearized around steady state. Analytical solutions are derived and are in good agreement with numerical results. Our model predicts the existence of a resonance on stiffness-stabilized surfaces with velocity-weakening: shear and velocity responses of the interface depend on the period of the external normal load and exhibit a peak response for a period denoted as the resonance period. The resonance is quite prominent when the spring stiffness is only modestly larger than its critical value. In Appendix B we show that this phenomenon also exists when periodic fluctuations of shear loading are considered, but for the sake of simplicity, mainly periodic normal stress perturbations will be discussed.

In the last part of this work, implications of our results for creeping faults are discussed. We show that periodic variations of the normal stress can influence the stability of creeping faults. Quasi-static stick-slip events are observed when the Dieterich law applies and are similar to "slow earthquakes" or creep bursts. We also discuss a possible extension of our results to the onset of (unstable) nucleating patches.

2. Model

The SB model consists of a rigid block (contact area set as unity) connected to a spring of stiffness k. The loading point is moving at constant velocity V_0 (Figure 1). The stiffness k is introduced to account for the elastic interaction of the sliding surface with the surrounding medium. The block has a mass m in order to incorporate the effect of inertia.

Frictional evolution is described by rate-and-state constitutive laws [*Dieterich*, 1979a, 1979b; *Ruina*, 1983] that successfully modeled a wide range of phenomena from rock friction laboratory measurements [*Dieterich*, 1979a, 1979b, 1981] to earthquake afterslip [*Marone et al.*, 1991]. These laws propose that friction τ can be described as

$$\tau = F(V, \psi, \sigma), \tag{1}$$

where τ is the friction force per surface unit, σ is the effective normal stress, $V = \dot{\delta}$ is the velocity, where δ is the position of the center of the block, and ψ is the state

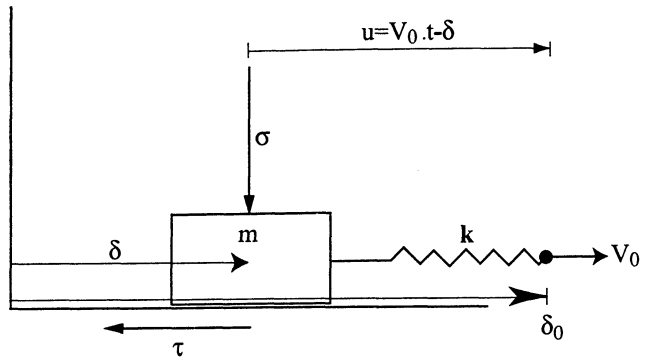

Figure 1. The spring-block model. Here τ is frictional strength, σ is effective normal stress, k is stiffness of the spring, V_0 is loading velocity, m is mass of the block, δ is position of the center of the block, δ_0 is position of the loading point, and $u = V_0 t - \delta$ is relative displacement between the loading point and the center of the block.

variable that describes the state of the sliding surface. *Ruina* [1983] has proposed the following form for the friction force τ:

$$\tau = \sigma\,[\mu_0 + a\,\ln(V/V_*) + \psi], \tag{2}$$

where μ_0 and a are experimentally determined constants and V_* is a normalizing velocity. Equation (2) is not defined for $V = 0$ but can be regularized as by *Rice and Ben-Zion* [1996] and *Ben-Zion and Rice* [1997] by appeal to an activated rate process interpretation [*Heslot et al.*, 1994] of the logarithmic term, including the effect of backward as well as forward activated steps. When the loading speed V_0 is equal to the normalizing velocity V_*, and there is steady sliding, ψ vanishes and the coefficient of friction is equal to μ_0. For the evolution of the state variable at constant normal stress σ, we will use $d\psi/dt = G(\psi, V)$. *Ruina* [1983] proposed a specific expression for this G function. In this study, we will mainly use this expression (hereinafter referred to as the Ruina or slip law), written as

$$G(\psi, V) = -(V/L)[\psi + b\ln(V/V_*)], \tag{3}$$

We may also use an alternative expression (hereinafter referred to as the Dieterich or ageing law), written as

$$G(\psi, V) = (bV_*/L)[\exp(-\psi/b) - V/V_*], \tag{4}$$

where b and L are two constants determined experimentally. Defining θ by $\psi = b\ln(V_*\theta/L)$, (4) becomes

$$\frac{d\theta}{dt} = 1 - V\theta/L \tag{5}$$

$$\tau = \sigma[\mu_0 + a\ln(V/V_*) + b\ln(V_*\theta/L)]. \tag{6}$$

This form is often used in the literature because when the slider is at rest ($V = 0$), θ can be interpreted as time t. This is why the state variable θ is often interpreted [*Dieterich*, 1979a, 1979b; *Baumberger et al.*, 1995] as the average age of the contacts.

This system has a steady state when the slider is moving uniformly at the loading speed V_0, under constant normal stress σ, and when $G(\psi_{ss}, V_0) = 0$. Both the Ruina and Dieterich laws lead in steady state to the same value of the state variable: $\psi_{ss} = -b\ln(V_0/V_*)$, and the friction coefficient ($\mu = \tau/\sigma$) is

$$\mu_{ss} = \mu_* + (a - b)\ln(V_0/V_*). \tag{7}$$

The derivative with time of the state variable ψ, $G(\psi, V)$, shows that the system evolves to steady state after it has slipped a length L which is therefore a characteristic length of friction, and often [*Dieterich*, 1979a, 1979b; *Baumberger et al.*, 1995] interpreted as the length to renew contacts between asperities. When b is greater than a, the steady state friction force is velocity-weakening and the system may be unstable. Stability analysis at constant normal stress [*Rice and Ruina*, 1983; *Gu et al.*, 1984; *Heslot et al.*, 1994] shows that this system exhibits a Hopf bifurcation. Infinitesimal perturbations from steady state sliding leave the system in stable slip when the stiffness k is greater than the critical stiffness k_c, while when the stiffness k is lower than the critical stiffness k_c, the system becomes unstable and stick slip is observed. *Rice and Ruina* [1983] showed that the critical stiffness is $k_c = k_0[1 + mV_0^2/(a\sigma L)]$ with $k_0 = \sigma(b - a)/L$. When a is greater than b, it is obvious that the system is always stable since the critical stiffness k_c is always negative. Alternatively, when k_c is replaced by a given stiffness k of a SB system, the equation defines the critical normal stress $\sigma_c = kL/(b-a) - mV_0^2/(aL)$ below which sliding is stable.

Quasi-static ($m = 0$) stability fields for finite perturbations in shear stress $\Delta\tau$ using the Ruina slip law [*Gu et al.*, 1984] show that if the normalized perturbation $\Delta\tau/\sigma a$ is greater than some value γ of order unity, the system can become unstable even in the stable domain. However *Ranjith and Rice* [1999] showed recently that such a result is not true for the ageing law (4). In the stable domain ($k > k_c$) the system is always stable independently of the magnitude of the perturbation. Figure 2 shows schematically these differences.

Experimental studies of friction on rock samples [*Linker and Dieterich*, 1992; *Richardson and Marone*, 1999] showed that the variation of the normal stress σ could be taken into account by adding a new term in the state variable evolution law. The derivative of ψ with time becomes

$$\frac{d\psi}{dt} = G(\psi, V) - \frac{\alpha}{\sigma}\frac{d\sigma}{dt}. \tag{8}$$

Figure 3 shows the influence of the parameter α for a step in normal stress on a stiff system which is initially in steady sliding. An infinitesimal step in normal stress $d\sigma$, applied instantaneously while V is maintained constant, would be accompanied by a step in shear strength $d\tau|_{V=\text{const}} = (\mu_{ss} - \alpha)d\sigma$. A derivation, and general-

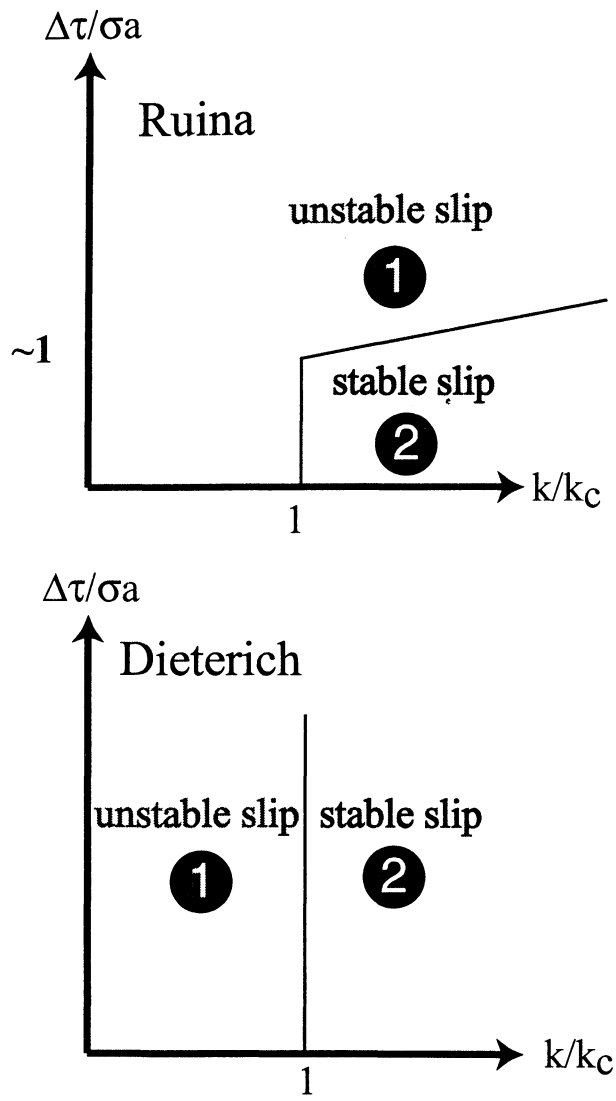

Figure 2. (top) Stability diagram of the spring-slider system for the Ruina slip law. For $k > k_c$ a finite perturbation can bring the system from domain 2 (stable slip or creep) to domain 1 (unstable slip or stick-slip). (bottom) Stability diagram of the spring-slider system for the Dieterich aging law. Note that unlike the Ruina law the system is always stable for $k > k_c$.

ization, of the last equality can be found in Appendix A. Since it is observed in the experiments mentioned above that an infinitesimal increase of normal stress ($d\sigma > 0$) implies also an infinitesimal increase of shear strength ($d\tau > 0$), the parameter α should lie between 0 and μ_{ss}. The amplitude of the response of the system to a step in normal stress σ decreases with increasing parameter α. When α is equal to the coefficient of friction in steady state μ_{ss}, there is no instantaneous change in shear strength. After this immediate response of the system, the shear strength τ evolves to a new steady state value related to the new value of the normal stress σ.

Experiments on friction of hard metals against a cutting tool material conducted at variable normal stress [*Prakash and Clifton*, 1993; *Prakash*, 1998], at slip rates of order 1 m s^{-1} (versus of order 1 μm s^{-1} of *Linker and Dieterich* [1992]), lead to a different formulation using the rate and state framework. These observations, obtained using a plate-impact shear-loading device, show continuous variation of shear strength following a step in normal stress, the coefficient of friction μ being still discontinuous (due to the step in σ). It is not clear if these differences are due to the experimental procedures employed, the far different timescales, the nature of the materials involved (homogeneous), or to the unavoidable presence of gouge in rock friction experiments. The *Linker and Dieterich* [1992] experiments may have been too slow and missed the (possible) continuity of τ. We can reconcile these two points of view if we take α in the Linker-Dieterich equations not as a constant but rather set $\alpha = \mu(V, \psi) = \tau/\sigma$ so that (8) transforms to

$$\frac{d\psi}{dt} = G(\psi, V) - \frac{\mu(\psi, V)}{\sigma}\frac{d\sigma}{dt}. \tag{9}$$

Then the Linker-Dieterich framework would imply no change in shear strength τ for a sudden ($dt \to 0$) change in the normal stress σ of arbitrary magnitude with V held constant. That is because $d\psi = d\mu$ in such circumstance, so that we have $d\mu = -\mu d\sigma/\sigma$, and hence $d(\mu\sigma) = 0$. Further studies should be carried out in order to settle these issues.

Three variables are needed to fully describe the system: The velocity $V(t)$ of the slider, the state variable $\psi(t)$, and the relative displacement of the slider compared to the loading point, which is $u(t) = V_0 t - \delta(t)$, where $\delta(t)$ is the position of the slider at time t. The

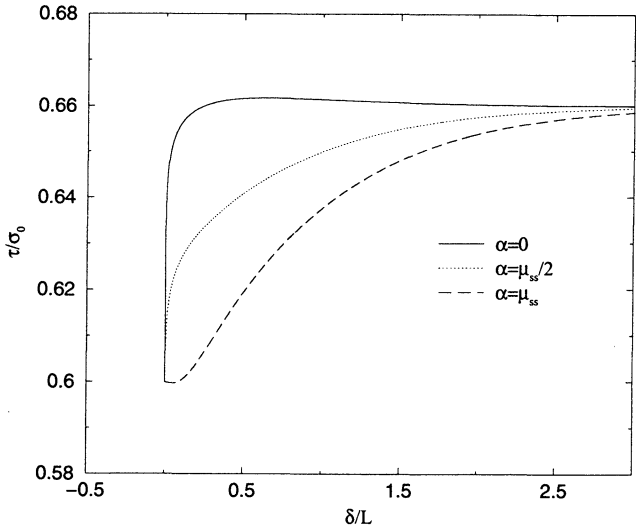

Figure 3. Effect of the α term on a step in normal stress σ. Shear stress τ/σ_0 plotted as a function of normalized displacement δ/L for the Ruina law. The parameters used are $a = 0.005$, $b = 0.008$, $V_0 = 10^{-9}$ m/s, $k = 10k_c$, and $\sigma_1 = 1.1\sigma_0$, where σ_0 and σ_1 are the initial and final normal stress. The instantaneous response of the system decreases with increasing α.

equations of motion of the spring-slider system evolving at variable normal stress σ are

$$\frac{du}{dt} = V_0 - V, \tag{10}$$

$$\frac{d\psi}{dt} = G(\psi, V) - \frac{\alpha}{\sigma}\frac{d\sigma}{dt}, \tag{11}$$

$$m\frac{dV}{dt} = ku - \tau, \tag{12}$$

where the shear strength τ is defined in (2) and where V_0 and $\sigma(t)$ are specified excitations.

We now consider variations of the normal stress σ with time t. The block is in steady state, and starting at $t = 0$, we apply a periodic perturbation in the normal stress σ of the form

$$\sigma(t) = \sigma_0[1 + \epsilon f(t)], \; |\epsilon f(t)| \ll 1. \tag{13}$$

To study the response, transient phases are not at first considered. Being in the stable domain, the effects of any perturbations of finite duration gradually vanish when those perturbations are removed. We therefore only consider perturbations for which the period is small compared to the total time during which they are applied. In this case, we can consider the forcing term $f(t)$ as permanent. In all the numerical runs performed here, we wait for the transient phase to disappear before reporting results.

The effects of periodic perturbations are studied both numerically and analytically. The case of an arbitrary perturbation of the normal stress is also considered but only using analytical results. The simplest type of periodic perturbation is $f(t) = \sin(2\pi t/T)$, T being the period of the perturbation. If $\Delta T_{\text{applied}}$ is the time during which the perturbation is applied, the criteria set in the paragraph above could be written as $\Delta T_{\text{applied}} \gg T$. We will use normalized quantities as often as possible. *Rice and Ruina* [1983] showed that the period of the spring-mass system at critical stiffness is $T_c = 2\pi\sqrt{a/(b-a)}(L/V_0)$. Therefore T/T_c will be the normalized period of the excitation $f(t)$.

To perform a full nonlinear analysis, we numerically integrate (10)-(12), using a Runge-Kutta algorithm [*Press et al.*, 1992] with fifth-order adaptive stepsize control. We take the normal stress as constant within each time step so that starting at time t_i it is σ_i and at time t_{i+1} it changes to σ_{i+1}. Equation (11) then requires that we change $\psi(t)$ from ψ_i to

$$\psi_{i+1} = \psi_i - \alpha \ln(\sigma_{i+1}/\sigma_i) \tag{14}$$

at time t_{i+1}, which is done before applying the Runge-Kutta algorithm to integrate the system of equations considering σ constant. This method allows us to account for the dependence of the state variable on σ in a simple manner and to consider a finite step in normal stress like in the experiments.

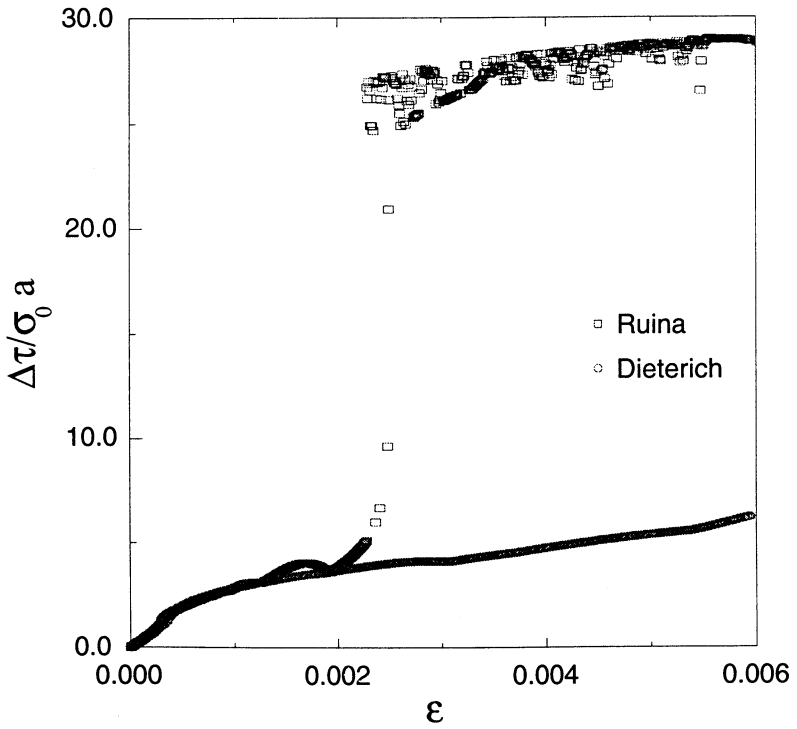

Figure 4. Normalized stress variation $\Delta\tau/\sigma_0 a$ as a function of the amplitude of the perturbation ϵ for the Dieterich (open circle) and the Ruina (open square) friction laws. The normalized stiffness $k/k_c = 1.1$, the excitation period $T/T_c = 1$, the parameter $\alpha = 0$, and the rest of the parameters are taken from Table 1. We see a step in the normalized stress drop for the Ruina law (due to the transition from stable to unstable slip), while for the Dieterich law the normalized stress drop appears more continuous as the perturbation ϵ is increasing.

Table 1. Parameters Used in This Study

Parameters	Values
a	0.005
b	0.008
L, μm	1
μ_*	0.6
V_*, m s^{-1}	10^{-9}
V_0, m s^{-1}	10^{-9}
σ_0, Pa	10^8
m, kg	1.0

3. Discrepancy Between "Slip" and "Ageing" Friction Laws

As discussed in section 2, the Dieterich and Ruina law behave distinctly for finite velocity perturbations at constant normal stress. For infinitesimal periodic fluctuations of the normal load, both laws give similar results. This is due to the fact that they both reduce to the same set of equations (as will be shown in section 4) when linearized around steady state. When finite perturbations are considered, the nonlinear terms can no longer be neglected and differences between these laws can be observed. The Ruina law is conditionally stable in the stable domain ($k > k_c$), while the Dieterich law is always stable despite the magnitude of the perturbation. When the amplitude of normal stress perturbations is increased, a transition from stable to unstable slip is observed in the case of the Ruina law and inertial effects have to be taken into account; otherwise, the problem has no solution. Stick slip is observed and the system does not behave quasi-statically. The inertial term mdV/dt is introduced in our numerical calculations to control the instability and limit the stress drop to a finite value. This term has no direct analog in continuum elastodynamics but plays a role comparable to the damping term $-GV/2\beta$ (where G is the shear modulus, V is the velocity, and β is the shear wave speed) derived from the elastodynamic theory [see, e.g., *Rice*, 1993; *Madariaga and Cochard*, 1994]. In the case of the Dieterich law the effect of inertia can still be neglected because unlike the slip law, it is stable to finite perturbations when the stiffness of the spring is greater than critical stiffness k_c.

Figure 4 displays the normalized stress drop $\Delta\tau/\sigma_0 a$ as a function of the amplitude of perturbation ϵ for the Ruina (open square) and the Dieterich (open circle) friction laws. The parameters used are taken from Table 1, the normalized stiffness $k/k_c = 1.1$, the normalized excitation period $T/T_c = 1$, and the parameter α is set to zero. The results are not qualitatively different when α varies. Note that for the stiffness k considered, the normal stress would have to be increased to $1.1\sigma_0$ to destabilize steady sliding; the entire range of ϵ considered in our plots is far smaller than the $\epsilon = 0.1$ to which that critical level would correspond.

The normalized stress drop exhibits a distinct step for the Ruina law compared to the Dieterich law, owing to its conditional stability toward finite perturbations. The normalized stress drop, for large amplitudes of perturbation ϵ, is always significantly larger in the case of the Ruina law. Figure 4 illustrates, as the perturbation ϵ becomes very small, the similar response of the Ruina and Dieterich laws. The quasi-static approximation for $k = 1.1k_c$ ceases to be valid for a perturbing amplitude ϵ larger than 2×10^{-3}, and the two curves begin to differ. In the discussion part of the paper, we propose a laboratory experiment based on these results that may be useful to study how well real surfaces conform to the predictions of these two laws.

The response in shear strength of the creeping surface is not only amplitude (ϵ) dependent but is also influenced by the period of the normal stress perturbations as shown on Figures 5a (for the Dieterich law) and 5b (for the Ruina law). Figures 5a and 5b display the normalized shear strength $\tau/(\mu_{ss}\sigma_0)$ as a function of the normalized time t/T_c for various periods, namely, $T = 0.1$, 1, and 10 T_c, the perturbation ϵ is equal to 10^{-2} and the stiffness k is equal to $1.1k_c$. The rest of the frictional parameters are given in Table 1. On Figures 5a and 5b, the response is clearly loading-period-dependent. Stable quasi-static oscillations are observed for both laws when the period is set to $0.1T_c$ or $10T_c$ (the response being higher for $10T_c$). The case $T = T_c$ is more interesting since stick slip is observed, showing that the normal stress perturbations have destabilized the fault. We will see in section 4 that the SB model presents a shear resonance (or peak response). When the stiffness is equal to $1.1k_c$, this occurs for periods of the normal stress perturbation close to T_c. This resonance is responsible for the transition from creep to stick-slip-like behavior. The stress drop associated with the Dieterich law is much lower than for the Ruina law, and the latter shows a periodic sequence of dynamical events (i.e., where inertia is important) while the former one presents an aperiodic distribution of quasi-static (i.e., inertia is always negligible) events, at least for the small $V_0 = 10^{-9}$ m/s we consider, although they constitute a quasiperiodic recurrence. When α is close to μ_{ss}, the Ruina law instead gives slightly aperiodic events. To summarize, the Dieterich law presents more complex behavior than the Ruina one and this feature has also been observed by *Rice and Ben-Zion* [1996, p. 3813] studying depth-variable crustal earthquake models, with the Ruina law "leading to periodically repeated events" and the Dieterich one sometimes "allowing apparently chaotic slip sequences of moderate and large earthquakes." In the light of our results, we may expect that the complexity observed by *Rice and Ben-Zion* [1996] using the Dieterich law might be enhanced if temporal fluctuations of the normal load are considered. This illustrates the need to test these two laws since they lead to important differences in the complexity of the generated events.

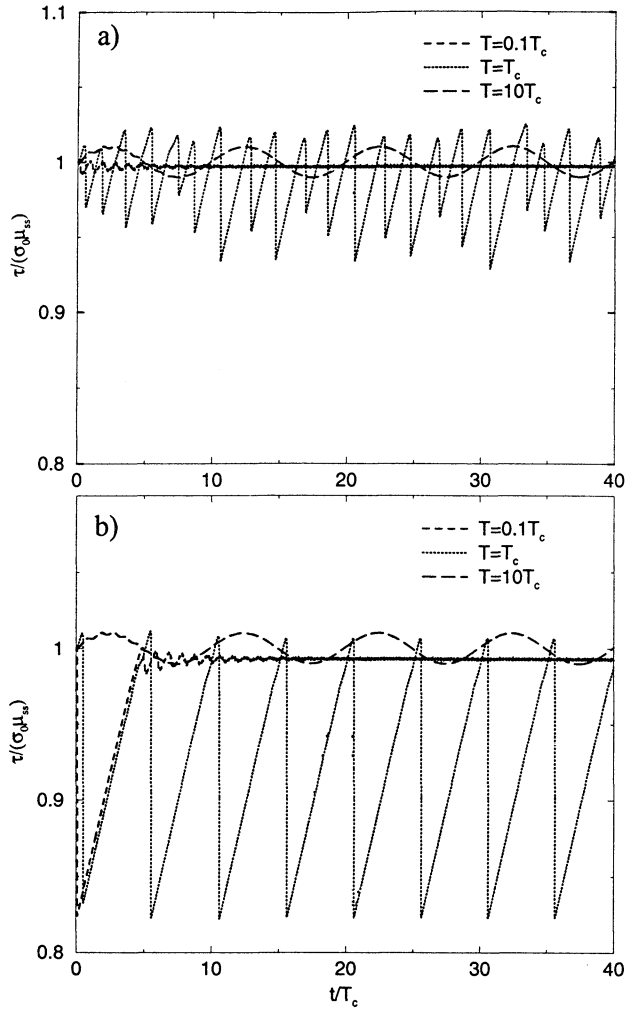

Figure 5. (a) Response in normalized shear stress $\tau_1/\sigma_0\mu_{ss}$ as a function of normalized time t/T_c using the Dieterich or "ageing" law for various periods of normal stress perturbation ($T = 0.1$, 1 and $10T_c$). Here α is equal to 0, the relative amplitude of the normal stress oscillation ϵ is set to 10^{-2}, and k/k_c is 1.1. The rest of the parameters are given in Table 1. The 0.1 (dashed) and $10T_c$ (long dashed) curves present quasi-static oscillations at the period imposed. The $T = T_c$ case shows a chaotic sequence of stick-slip events. However, the spring-slider system is behaving in a quasi-static way for the low V_0 we use, owing to the stability of the Dieterich law in the $k > k_c$ region. (b) Same as in Figure 5a for the Ruina law. For $T = T_c$ the slip law exhibits periodic stick-slip events, but unlike the Dieterich law, inertia can not be neglected. The system shows a transition from a quasi-static to an inertia-dominated regime due to the conditional stability of the Ruina law. Note that the stress drop is higher for the Ruina than for the Dieterich friction law and that the highest value of frictional strength is greater than its steady state value $\tau_{ss} = \sigma_0\mu_{ss}$ for the Dieterich law, while for the Ruina slip law this peak response occurs near τ_{ss}.

4. Linear Perturbation Analysis

4.1. Case of Sinusoidal Forcing

We consider first the quasi-static case (setting the mass equal to zero: $m = 0$) and develop a linear perturbation analysis for a system which is sliding in steady state but subjected to a small periodic fluctuation of the normal stress in the form

$$\sigma(t) = \sigma_0 + \sigma_1 \sin(\omega t) = \sigma_0 + \mathrm{Im}[\sigma_1 \exp i\omega t], \quad (15)$$

where $\omega = 2\pi/T$ and $\sigma_1/\sigma_0 = \epsilon \ll 1$. A general derivation including periodic fluctuations of the shear loading is given in Appendix B.

As mentioned in section 3, we ignore transients and determine the periodic response. The transients will decay and be unimportant when the stiffness k is greater than the critical stiffness $k_c = \sigma_0(b-a)/L$. On the other hand, if the stiffness k is lower than the critical stiffness k_c, the transients have exponential growth and there will be no (stable) steady state to perturb. We are seeking for solutions of the linearized system (10)-(12) together with (2). Because of the linearization, we have to look for solutions which vary temporally in a manner identical to the perturbation in $\sigma(t)$. It is also important to note that since the perturbation is imposed, T and therefore ω are imposed and real quantities.

Thus we assume $k > \sigma_0(b-a)/L$ and solve the linearized equations of the problem in the form

$$u = u_0 + \mathrm{Im}[u_1 \exp(i\omega t)], \quad (16)$$

$$\psi = \psi_0 + \mathrm{Im}[\psi_1 \exp(i\omega t)], \quad (17)$$

$$\tau = \tau_0 + \mathrm{Im}[\tau_1 \exp(i\omega t)], \quad (18)$$

$$V = V_0 + \mathrm{Im}[V_1 \exp(i\omega t)], \quad (19)$$

where all of u_1, ψ_1, τ_1, and V_1 are small complex quantities to be determined. Both the Ruina (slip) and Dieterich (ageing) forms of constitutive law discussed, including the Linker-Dieterich framework for variable normal stress influence, reduce to the same linearized set of equations so the results obtained in the rest of the text, unless specified, are common to the Dieterich and Ruina laws. Thus the expression for τ in (2) reduces to

$$\tau_1 = \mu_{ss}\sigma_1 + a\sigma_0 V_1/V_0 + \sigma_0\psi_1, \quad (20)$$

whereas the two forms of the state evolution both linearize to

$$i\omega\psi_1 = -(V_0/L)(\psi_1 + bV_1/V_0) - i\alpha\omega\sigma_1/\sigma_0. \quad (21)$$

The equation of equilibrium (12) (when $m = 0$) is

$$\tau_1 = ku_1, \quad (22)$$

and the spring elongation equation (10) yields

$$i\omega u_1 = -V_1. \quad (23)$$

The $i\omega$ comes from time derivatives, and we dispense with writing the imaginary symbols $\mathrm{Im}[(...)_1 \exp(i\omega t)]$. It is elementary to solve these four equations for u_1, ψ_1, τ_1, and V_1. The result for τ_1 is conveniently normalized

by $\mu_{ss}\sigma_1$, which would be the nominal change in shear strength if we neglected the rate and state effects. Thus introducing the dimensionless pulsation $q = \omega L/V_0 = 2\pi L/V_0 T$, we obtain

$$\frac{\tau_1}{\mu_{ss}\sigma_1} = \frac{1 + iq(1 - \alpha/\mu_{ss})}{[1 - \frac{a\sigma_0 q^2}{kL}] + iq[1 - \frac{(b-a)\sigma_0}{kL}]}. \quad (24)$$

When inertia is considered ($m \neq 0$), (22) becomes

$$\tau_1 + i\omega m V_1 = k u_1, \quad (25)$$

and (24) transforms to

$$\frac{\tau_1}{\mu_{ss}\sigma_1} = \frac{1 + iq(1 - \alpha/\mu_{ss})}{[1 - \frac{a\sigma_0 q^2}{(k - m\omega^2)L}] + iq[1 - \frac{(b-a)\sigma_0}{(k-m\omega^2)L}]}. \quad (26)$$

As already noted by *Rice and Ruina* [1983], including inertia is equivalent to replace k by $k - m\omega^2$ in the results obtained for $m = 0$ as can be seen by comparing (24) with (26).

Equation (24) is, in fact, in the same form as that for a harmonically forced system consisting of a mass M, a spring of stiffness K and a damper of viscous damping C_d on which two forces are acting: A periodic force $f(t) = f_0 \,\mathrm{Im}\,[\exp(i\omega t)]$ and another force of the type $\kappa df(t)/dt$. If the system position is $x(t) = x_0 + \mathrm{Im}\,[x_1 \exp(i\omega t)]$, the "transfer function" x_1/f_0 is equal to $(1 + i\omega\kappa/f_0)/(K - M\omega^2 + iC_d\omega)$. The viscous damping C_d is similar to $1 - k_c/k$, so that the case $k > k_c$ (as we assume here) is analogous to positive damping and vice versa.

So far, we have considered real values of ω since the frequency of motion was imposed. If we now let ω be a complex number and σ_1 go to zero, then our results could be used to perform a stability analysis of a slider under a constant normal stress, and to solve for the critical stiffness value k_c. Because of (24) the values of the dimensionless frequency q that make the denominator of (24) vanish suggest solutions of the form $\exp(iqV_0 t/L)$. The zeros of the denominator are given by

$$\frac{2a\sigma_0 q}{L} = i[k - \frac{(b-a)\sigma_0}{L}] \pm \sqrt{\frac{4a\sigma_0 k}{L} - [k - \frac{(b-a)\sigma_0}{L}]^2}. \quad (27)$$

Stable solutions correspond to $\mathrm{Im}\,(q)$ greater than zero. So, when the stiffness k is greater than $k_c = (b-a)\sigma_0/L$ (or when, for a given k, stress σ_0 is less than $kL/(b-a)$), the system is stable. This confirms the well-known stability result of *Ruina* [1983] and *Rice and Ruina* [1983]. For analysis of the dynamical regime ($m \neq 0$) the stiffness k is replaced by $k - m\omega^2$.

We will show in section 5 that the response of the block shows a peak response for a period that will be denoted as the resonance period T_r. Figure 6 displays this resonance in the shear stress oscillation as a function of the normalized period of normal stress perturbations T/T_c for $a = 0.005$, $b - a = 0.003$, $\epsilon = 10^{-3}$, and various values of the stiffness k ($k = 1.1k_c$, $1.5k_c$, and $5k_c$). It shows that the numerical (symbols) and the analytical (solid lines) values are in very good agreement.

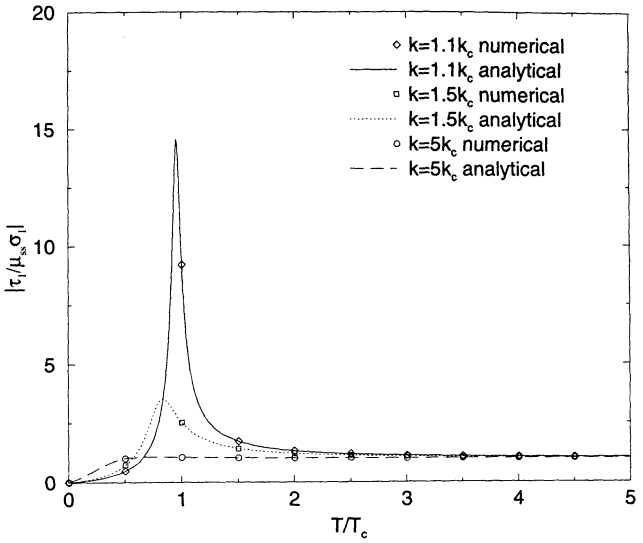

Figure 6. Normalized modulus of the shear stress versus normalized period of the excitation T/T_c for $\alpha = \mu_{ss}/2$ and $k = 1.1$, 1.5, and $5k_c$. The parameters used are given in the set of parameters of Table 1. The sharp peak shows the existence of a resonance. The peak response is decreasing with increasing stiffness.

4.2. Case of an Arbitrary Forcing (Arbitrary *f(t)*)

Let the perturbation in normal stress be given by

$$\sigma_1(t) = (1/2\pi)\int_{-\infty}^{+\infty} \exp(i\omega t)\tilde{\sigma_1}(\omega)d\omega, \quad (28)$$

where $\tilde{\sigma_1}(\omega)$ is the Fourier transform of $\sigma_1(t)$,

$$\sigma_1(\omega) = \int_{-\infty}^{+\infty} \exp(-i\omega t)\sigma_1(t)d\omega, \quad (29)$$

and we note that for transient response we would set $\sigma_1(t) = 0$ for all $t < 0$. In section 4.1 we considered excitation in the form $\sigma_1 \exp(i\omega t)$ and showed how to compute response perturbations $\tau_1 \exp(i\omega t)$, $V_1 \exp(i\omega t)$, $\psi_1 \exp(i\omega t)$, and $u_1 \exp(i\omega t)$. Let us rewrite the result of that calculation as

$$\begin{pmatrix} \tau_1 \\ V_1 \\ \psi_1 \\ u_1 \end{pmatrix} \exp(i\omega t) = \begin{pmatrix} F_1(\omega) \\ F_2(\omega) \\ F_3(\omega) \\ F_4(\omega) \end{pmatrix} \sigma_1 \exp(i\omega t). \quad (30)$$

Equation (24) gives

$$F_1(\omega) = \mu_{ss}[1 + i(\omega L/V_0)(1 - \alpha/\mu_{ss})]/ [(1 - a\sigma_0\omega^2 L/kV_0^2) + i(\omega V_0/L)(1 - (b-a)\sigma_0/kL)], \quad (31)$$

equation (22) leads to

$$F_4(\omega) = F_1(\omega)/k, \tag{32}$$

equation (23) leads to

$$F_2(\omega) = -i\omega F_1(\omega)/k, \tag{33}$$

and, finally, equation (21) gives

$$F_3(\omega) = \frac{i\omega(bF_1(\omega)/kL - \alpha/\sigma_0)}{i\omega + V_0/L}. \tag{34}$$

These are for the quasi-static case and can be extended by replacing k by $k - m\omega^2$ to include inertial dynamics. Then, if we replace σ_1 by $\tilde{\sigma_1}(\omega)d\omega/2\pi$ and integrate such solutions over all ω, the response to a general perturbation history $\sigma_1(t)$ is

$$\begin{pmatrix} \tau_1(t) \\ V_1(t) \\ \psi_1(t) \\ u_1(t) \end{pmatrix} = \frac{1}{2\pi} \times \int_{-\infty}^{+\infty} \begin{pmatrix} F_1(\omega) \\ F_2(\omega) \\ F_3(\omega) \\ F_4(\omega) \end{pmatrix} \tilde{\sigma_1}(\omega) \exp(i\omega t) d\omega. \tag{35}$$

4.3. Quasi-Static Slip Between Deformable Elastic Continua

The development here is for the single degree of freedom SB system. However, the quasi-static ($m = 0$) form of our equations also has an interpretation for sliding on a planar surface between two identical deformable elastic continuum layers, extending infinitely in the x direction, provided that we focus on perturbations of a given spatial wavenumber ξ [see, e.g., *Rice and Ruina*, 1983]. That is, letting x be the coordinate along the interface which is either parallel (in-plane slip case) or perpendicular (antiplane slip) to the slip direction, we may consider a perturbation of a steady sliding state by a space-time perturbation of normal stress in the form

$$\sigma(x,t) = \sigma_0 + \mathrm{Im}[\sigma_1 \exp(i\xi x) \exp(i\omega t)] \tag{36}$$

analogous to (15). The response of the system can be written similarly to (16)-(19),

$$\begin{pmatrix} u(x,t) \\ \psi(x,t) \\ \tau(x,t) \\ V(x,t) \end{pmatrix} = \begin{pmatrix} 0 \\ \psi_0 \\ \tau_0 \\ V_0 \end{pmatrix} + \mathrm{Im}\left[\begin{pmatrix} u_1 \\ \psi_1 \\ \tau_1 \\ V_1 \end{pmatrix} \exp(i\xi x) \exp(i\omega t) \right], \tag{37}$$

where $-u(x,t)$ is now the slip along the interface, in addition to the uniform slip $V_0 t$, due to perturbation of the sliding state. These quantities satisfy the same system of (20) to (23), except that the parameter k must be regarded as the elastic-stiffness at wavenumber ξ named as $K_{eq}(\xi)$. For two elastic half-spaces (i.e., when ξ times the layer thicknesses is much less than 1), $K_{eq}(\xi) = G|\xi|/2(1-\nu)$ for in-plane slip and $K_{eq}(\xi) = G|\xi|/2$ for antiplane slip, where G is the elastic shear modulus and ν the Poisson ratio. Expressions for k for sliding elastic layers of finite thickness are given by *Rice and Ruina* [1983] and *Horowitz and Ruina* [1989].

Using the appropriate expression for k, results for the quasi-static SB (equations (24) and (35)) hold for perturbations at wavelength ξ but arbitrary time-dependent normal stress perturbations of two sliding half-spaces or layers. Thus, to describe perturbation in a single wavenumber mode between elastic half-spaces, we can simply reinterpret k/k_c in our plots, for quasi-static linearized perturbation results, as $|\xi|/|\xi_c|$ where ξ_c is the critical wavelength defined, e.g., in antiplane strain, by $G|\xi_c|/2 = k_c$. The half wavelength π/ξ_c can be interpreted roughly as the nucleation length [see, e.g., *Rice*, 1993] and represents the minimum size above which slip becomes unstable.

There is no clear fault interpretation for sliding continua of the SB analysis with inertia ($m > 0$); such cases must be examined on the basis of solutions to the elastodynamic wave equations like done, for instance, by *Rice and Ruina* [1983] for the antiplane case.

5. Shear Stress Resonance

The denominator of (24) vanishes for a stiffness $k = k_c$ and $q = q_c = \sqrt{(b-a)/a}$ leading to an excitation period $T = T_c = 2\pi\sqrt{a/(b-a)}L/V_0$, the period at instability identified by Rice and Ruina [1983] when $k = k_c$. The ratio $\tau_1/\mu_{ss}\sigma_1$ is unbounded at that frequency. The system at critical stiffness shows a variation of its response amplitude in shear strength as the period of excitation varies and presents a maximum (and infinite response) for $T = T_c$. We recognize such a behavior as a resonance phenomenon.

Similarly, when the stiffness k is greater than the critical stiffness k_c, there is an amplified response, but the resonance is bounded.

If we write the normalized change in shear strength $\tau_1/\mu_{ss}\sigma_1$ in (24) as

$$\tau_1/\mu_{ss}\sigma_1 = \rho_\tau \exp(-i\gamma_\tau), \tag{38}$$

it can be easily derived that

$$\rho_\tau = \sqrt{\frac{1 + q^2(1-\alpha/\mu_{ss})^2}{(1 - a\sigma_0 q^2/kL)^2 + q^2(1-k_c/k)^2}} \tag{39}$$

$$\tan\gamma_\tau = q\frac{(1-\frac{k_c}{k}) - (1-\frac{a\sigma_0 q^2}{kL})(1-\frac{\alpha}{\mu_{ss}})}{1 - \frac{a\sigma_0 q^2}{kL} + q^2(1-\frac{k_c}{k})(1-\frac{\alpha}{\mu_{ss}})}. \tag{40}$$

The modulus of the normalized shear stress change ρ_τ is useful to illustrate this resonance as the period T varies. When the resonance exists, $\rho_\tau(T)$ has a maximum for a period $T = T_r$ called the resonance period. This has been illustrated in Figure 6. When the period of excitation T goes to zero ($q \to \infty$), the normalized change in shear stress goes to zero. T is too short for significant changes in spring extension to accumulate over a single period, and τ is then equal to $\tau_0 = \tau_{ss}$. When the period of excitation T becomes very large compared to the characteristic time of the evolution of friction L/V_0 (i.e. $q \to 0$), the modulus of the normalized change in shear strength goes to unity: The system responds as if it was at "constant" normal stress (i.e., variations of the normal stress are slow); it has time to adapt to the evolution of the normal stress. Between these two asymptotic values of the modulus of the shear stress changes, a maximum and therefore a resonance may exist. The resonance leads to a peak response up to 15 times larger than its value at steady state when $k = 1.1k_c$ and $\alpha = \mu_{ss}/2$ (see Figure 6).

Examination of (39) shows that the magnitude of the shear stress response decreases with increasing α. This illustrates again the stabilizing effect of this term to normal stress perturbations.

The boundary between creep and stick slip behavior is highly influenced by the existence of the resonance: When at shear resonance, initially creeping fault will exhibit stick slip for lower amplitudes of the normal stress fluctuations than for any other periods (see section 3).

6. Phase Lag Between Shear Stress and Normal Stress

Let us now consider the phase lag γ_τ between the fluctuations of the shear and normal stresses. Using (38) together with (18), we obtain

$$\tau = \mu_{ss}\sigma_0[1 + \epsilon\rho_\tau \sin(\omega t - \gamma_\tau)]. \qquad (41)$$

When the period of excitation T becomes very long compared to the characteristic time of the evolution of friction L/V_0 (i.e., when $q \to 0$), then $\gamma_\tau \simeq 0$ (see (40)) and the system responds in phase to the external excitation of the normal stress $\sigma(t)$.

When the period of excitation T goes to zero ($q \to \infty$), two cases have to be considered. If α differs from the value of the coefficient of friction in steady state μ_{ss}, then $\gamma_\tau \simeq \pi/2$, but when the parameter α is equal to μ_{ss}, we find that $\gamma_\tau \simeq \pi$. For very low periods of excitation and $\alpha = \mu_{ss}$ the shear stress is directly out of phase with the normal stress.

Another property of the system when the normal stress fluctuates at frequency q_c is that the phase lag of the shear stress does not depend on the stiffness of the spring (see (40) at $q = q_c$). In other words, the elastic properties of the surrounding medium do not influence the phase lag between the normal and the shear stress. Nevertheless, elastic properties still influence the magnitude of the response.

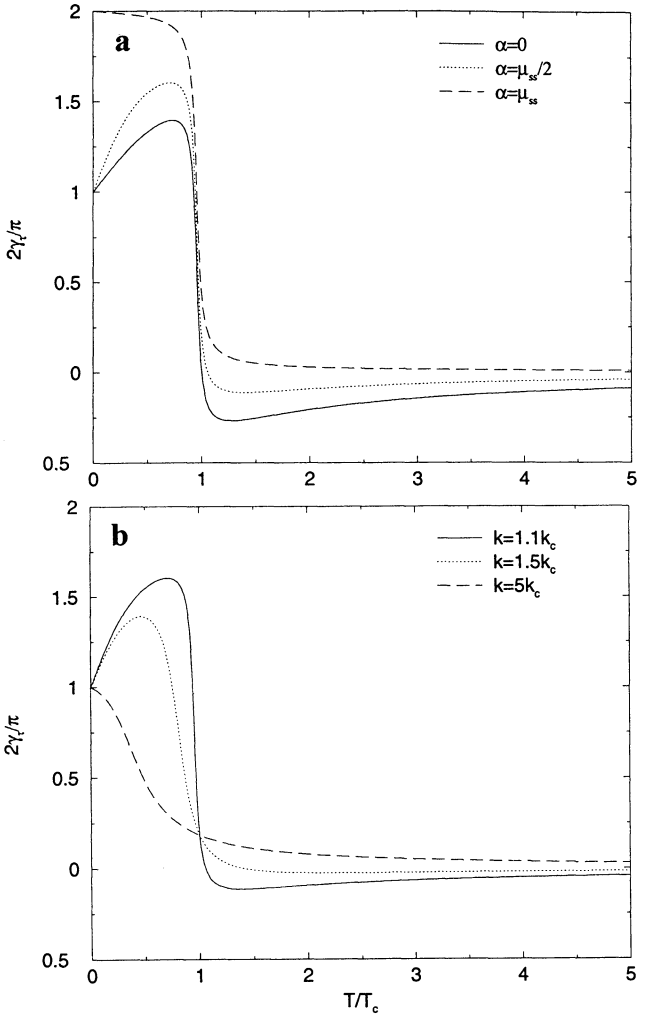

Figure 7. (a) Normalized phase lag $2\gamma_\tau/\pi$ between shear and normal stress oscillations versus normalized period of the excitation T/T_c for $k = 1.1k_c$ and $\alpha = 0$, $\mu_{ss}/2$, and μ_{ss}. The parameters used are given by the set of parameter in Table 1. (b) same as in Figure 7a for α set to $\mu_{ss}/2$ and various stiffness ($k = 1.1$, 1.5, and $5k_c$).

The same kind of analysis can be carried out to study the influence of the α parameter. As expected, the phase lag is always increasing with increasing α. This is an illustration of the stabilizing effect of the Linker-Dieterich α parameter which acts against the variation of normal stress.

Figures 7a and 7b display the phase lag as a function of the normalized period of excitation T/T_c for various values of the normalized stiffness k/k_c (1.1, 1.5, and 5) and α (0, $\mu_{ss}/2$ and μ_{ss}) when $a = 0.005$, $b - a = 0.003$. As mentioned above, the $k = 1.1$, 1.5 and $5k_c$ curves intersects at $T = T_c$ for all α. When $\alpha = \mu_{ss}$ (see Figure 7a), the phase lag is always positive and never reaches 0. The shear stress is never in phase with the normal stress due to the counter reaction of the α parameter toward perturbations of the normal load.

For stiffnesses close to the critical stiffness ($k = 1.1$ and $1.5k_c$ curves of Figure 7b), the phase lag shows an abrupt variation as T/T_c crosses unity (this drop is equal to π when $\alpha = \mu_{ss}$). This is similar to the spring (stiffness K)-mass (M) system in the absence of frictional effects and subject to a periodic variations of the driving force of the form $F_0 \exp(i\omega t)$.

7. Velocity Resonance

It is also of interest to look at variations of the slider velocity during creep with oscillations of the normal load by studying the fluctuations of speed $V_1(t)$. It can be easily seen from (22) and (23) that $V_1 = -i\omega\tau_1/k$. Therefore, if we write

$$V_1/V_0 = \rho_V \exp(-i\gamma_V), \tag{42}$$

the magnitude ρ_V and the phase lag γ_V with respect to the normal stress fluctuations are related to shear stress magnitude ρ_τ and phase lag γ_τ as

$$\rho_V = \frac{q\mu_{ss}\sigma_1\rho_\tau}{kL}, \tag{43}$$

which shows that the shear stress and velocity do not exhibit their highest response for the same period of normal stress fluctuations (since $\rho_V \sim q\rho_\tau$).

$$\gamma_V = \gamma_\tau + \pi/2. \tag{44}$$

So shear τ fluctuations of the slider are extremal when the velocity V fluctuations vanish, and vice versa, and the speed of the slider can be written as

$$V(t) = V_0 + \frac{\tau_{ss}\rho_\tau\epsilon V_0 q}{kL}\cos(\omega t - \gamma_\tau). \tag{45}$$

When the period of excitation T is much greater than the characteristic time L/V_0 of evolution of friction ($q \to 0$), then the speed magnitude ρ_V goes to 0. The system is sliding at constant steady state velocity V_0.

When T is small compared to L/V_0 ($q \to \infty$), ρ_V approaches $V_0\epsilon(\mu_{ss} - \alpha)/a$. Figure 8 shows the normalized velocity magnitude $kL\rho_V/(\mu_{ss}\sigma_1 V_0) = q\rho_\tau$ for various values of the normalized stiffness k/k_c (1.1, 1.5 and 5) and $\alpha = \mu_{ss}/2$ when $a = 0.005$, $b - a = 0.003$ (see Table 1).

As for the case of the shear stress response, the magnitude of the velocity response decreases with increasing α (see (43) together with (39)) showing again the stabilizing effect of the α parameter for normal stress variations. We also verified that at resonance, the velocity was a decreasing function of the stiffness and that the higher the parameter α, the lower is the response of the velocity.

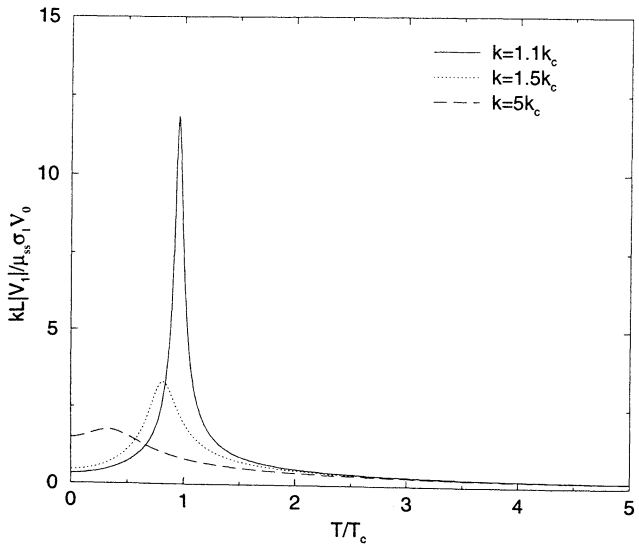

Figure 8. Normalized modulus of the velocity $kL\rho_V/\mu_{ss}\sigma_1 V_0$ as a function of the normalized period of the excitation T/T_c for various stiffnesses ($k = 1.1$, 1.5, and $5k_c$) and $\alpha = \mu_{ss}/2$ fixed. The peak velocity response decreases for increasing stiffness.

8. Implications for Faults

8.1. Three Characteristic Parameters

Three main parameters characterize the resonance phenomenon: (1) The critical stiffness $k_c = \sigma_0(b-a)/L$. (2) The period of the SB system at critical stiffness $Tc = 2\pi\sqrt{a/(b-a)}(L/V_0)$. (3) The critical magnitude of the normal stress perturbations ϵ_c for destabilization.

A rough estimate of the latter can be made by finding the ϵ which would predict so large a $|V_1|$ that it equals the unperturbed velocity V_0. That is clearly outside the range of the linearized analysis but predicts a value in reasonable accord with our simulations. Thus setting $\rho_V = 1$ when $T = T_c$ and setting $k = k_c$ everywhere except in the term $1 - k_c/k$, we estimate that a value of ϵ sufficient to destabilize steady sliding at the peak resonance is

$$\epsilon_c \simeq \frac{b-a}{\mu_{ss}}\frac{1 - k_c/k}{\sqrt{1 + (1-\alpha/\mu_{ss})^2(b-a)/a}}. \tag{46}$$

This gives $\epsilon_c \simeq 0.04$ to $0.05(1 - k/k_c)$ for the parameter values in Table 1, with the range corresponding to choice of $\alpha = 0$ to $\alpha = \mu_{ss}$. Thus $\epsilon_c \simeq 0.004$ for the cases we studied in Figures 4 and 5, with $k = 1.1k_c$, which is in reasonable agreement with what we find by simulations.

Estimates of these parameters k_c, T_c, ϵ_c require the knowledge of the frictional parameters a, b, and L, the value of the mean normal stress σ_0, the loading velocity V_0 and, for ϵ_c, the stiffness k.

The frictional parameters a and b of a fault vary along depth due for instance to temperature variations. Using data on temperature dependence of $a-b$ for granite under hydrothermal conditions, *Blanpied et al.* [1991] converted them to variations of $a-b$ with depth as based on a Lachenbruch-Sass San Andreas fault geotherm. They found that for depth between 0 and -2 km, $a > b$ (velocity strengthening regime), and $b > a$ (velocity-

weakening regime) for depth between -2 *km* and -14 *km*, with $b - a \simeq 4 \times 10^{-3}$, similar to what we use in Table 1. Below -14 *km* the fault is again velocity strengthening. *Blanpied et al.* [1991] did not report the value of a, but if we choose a over the velocity-weakening range as roughly 0.005 to 0.015 (values consistent with other laboratory experiments on friction), the $\sqrt{a/(b-a)}$ factor varies from 1.1 to 1.9, which is not significantly different from 1.3 based on Table 1. Smaller values of $b - a$ should, of course, be expected near the transition between the velocity-strengthening and weakening regime, that is, for depths of -2 *km* or -14 *km* where $b - a$ crosses zero in changing sign. Lateral variations of fault friction may also be considered as by *Boatwright and Cocco* [1996]. They propose that faulting behavior is divided into four categories: Strong and weak seismic fields and compliant as well as viscous fields. The two latter involve a velocity strengthening regime ($b < a$) and so only the first two categories should apply to our model. Strong and weak seismic fields are velocity-weakening ($b > a$) regions. The weak areas are close to velocity neutral ($b \simeq a$), while the strong portions of the fault exhibit significant velocity-weakening. *Boatwright and Cocco* [1996] discussed the presence of microearthquakes on the creeping section of the San Andreas fault suggesting that this area is a mosaic of velocity-weakening and strengthening regions whose $b - a$ values highly fluctuate. This raises the possibility that faults may be composed of many parts showing different frictional behavior.

Concerning the parameter L, typical laboratory values of the order of 1 μm. However, these values might possibly not be appropriate to describe earthquake faults. *Marone and Kilgore* [1993] found a scaling between L and the thickness w of the zone of localized shear strain which led them, based on field estimate of w for the San Andreas fault, to estimate values of L of the order of 1 mm. Nevertheless, for the velocity-weakening faults of concern here, shear is expected to be highly localized rather than occupying the entire thickness w, and such scaling is uncertain. Higher L (even of the order of a meter) has been suggested by waveform inversion but may be biased by the inversion method as pointed out by *Guatteri and Spudich* [2000].

It is normally assumed that the effective stress σ_0 increases linearly with depth. At a given depth, normal stress may vary due, for instance, to geometric changes of the fault surface, or to the presence of fluids at higher than hydrostatic pore pressure. For such regions the effective normal stress may be much reduced from the standard estimate based on lithostatic pressure minus hydrostatic pore pressure.

In extending the results to natural faults the SB model is not directly applicable, and we have to describe the problem in terms of nonuniform slippage on a surface in an elastic continuum. That lies beyond our present scope, but, approximately, we may discuss results in terms of an equivalent stiffness K_{eq} for a wavenumber ξ (see section 4.3). We identify the length h of a slipping fault segment as a half wavelength, so that $k = K_{eq}(\pi/h) = \pi G/2h$.

8.2. Resonance Phenomenon on Faults

Our results have clear implications for laboratory study of friction and tests of proposed constitutive relations. Here we examine the possibility that the resonance phenomenon, and associated destabilization of what would otherwise be stiffness-stabilized slip, could be relevant to natural earthquakes. We have three requirements for estimating the influence on faults of the resonance phenomenon:

First, the excitation period T must be close to the critical period $T_c = 2\pi\sqrt{a/(b-a)}(L/V_0)$, which constrains V_0 (to the value given later in (48)) for fixed frictional parameters a, b, and L and imposed period T. Any fault segment which appears to be "locked" between seismic events must ultimately slide in such a speed range on its way towards the next instability. If it resides close to that velocity for enough periods, there is the possibility of resonance. Of course, the range of slip rate V_0 is influenced by the choice of the value of the frictional parameters, and we discuss estimates below. The requirement $T = T_c$ can also be achieved by a random loading (e.g., by stress changes from nearby earthquakes in an aftershock sequence) if it has sufficient spectral strength at the period T_c.

The second requirement is that the stiffness k must not be too far above (or normal stress too far below) the critical value. That is, $k \simeq k_c$, while $k > k_c$. At critical stiffness k_c the length h_c of the slipping patch approximately satisfies $k_c = K_{eq}(\pi/h_c)$. This leads to $h_c = \pi GL/2(b-a)\sigma_0$, which is like the parameter h^* of *Rice* [1993]. The slipping area should exhibit stable slip, which gives a constraint $h < h_c$ on the size of the patch, but to meet the second requirement for resonance, h must be close to that upper limit h_c. Taking $b - a = 0.003$, as in Table 1, $G = 30$ GPa, and $L = 1$ to $10\,\mu$m, we get $h_c = 0.15$ to 1.5 m when $\sigma_0 = 100$ MPa. This range for h_c increases when the effective stress is lower; for example, it is 1.5 to 15 m when $\sigma_0 = 10$ MPa and 15 to 150 m in the extreme case, perhaps unrealistic, when $\sigma_0 = 1$ MPa. The scaling of h_c is with $L/(b-a)$ at a given σ_0, and unfortunately, those parameters for tectonic faults, and thus h_c too, are only weakly constrained at present.

We can imagine three scenarios in which there might be such stiffness-stabilized fault patches, which could slip for a long time at nearly constant rate:

1. The creeping patch is surrounded by velocity-strengthening regions which show stable slip. (This is the case of small velocity-weakening regions on a creeping fault. In that case, the average slip velocity is easy to estimate and is consistent with the nearby creep velocity (say, V_0 of the order of 10 mm/yr).)

2. The patch is a finite fault segment (with unruptured ends) of sufficiently small length.

3. The patch is a region of locally low σ_0 along a velocity-weakening fault, which is presently loaded to a level of overall shear stress so that only that region slips while its surroundings, at higher σ_0, are still locked.

The last two scenarios involve a small creeping region of size $h < h_c$ surrounded by nonslipping, or at least currently locked, areas. We may note that the slip rate under a remotely applied shear stressing rate $d\tau/dt$ is then of order $h(d\tau/dt)/G$. Since h must be near the nucleation length $h_c = \pi GL/2(b-a)\sigma_0$ for resonant destabilization, this yields a slip rate

$$V_0 = h_c(d\tau/dt)/G = \pi L(d\tau/dt)/2(b-a)\sigma_0. \quad (47)$$

To meet the first requirement (T near T_c), the loading velocity must also satisfy

$$V_0 = 2\pi\sqrt{a/(b-a)}L/T, \quad (48)$$

which directly arises from the definition of T_c. For the first and second requirements to be compatible with one another, (47) and (48) lead to

$$T(d\tau/dt) = 4\sqrt{a(b-a)}\sigma_0. \quad (49)$$

Note that L has canceled out of this condition. Assuming, as above, that a lies in the range from 0.005 to 0.015, while in the velocity-weakening regime, typical values of $b-a$ range from 0.002 to 0.004, (49) becomes $T(d\tau/dt) \simeq 0.02\sigma_0$. The factor 0.02 is the midpoint of a range from 0.01 (when $a = 0.005$ and $b-a = 0.002$) to 0.03 (when $a = 0.015$ and $b-a = 0.004$).

In areas of active tectonics near plate margins we may assume that, roughly, $d\tau/dt \simeq 0.002 - 0.02$ MPa yr^{-1}, which is consistent with having a major earthquake of 3 MPa average stress drop every 150 to 1500 years. Thus the first two requirements for resonance will be consistent only if the excitation period and normal stress are related by

$$T \simeq (1 \text{ to } 10)\sigma_0 \text{yr/MPa}. \quad (50)$$

Knowing the period of the normal stress variations, (50) can be used to obtain a reasonable range of the mean normal stress σ_0 that would allow resonance. We shall see in section 8.3 that it precludes the possibility that resonance could occur in scenarios 2 and 3 above in essentially any tectonic setting.

The third requirement for estimating the influence of the resonance phenomenon concerns destabilization. If the magnitude of the perturbation ϵ is large enough $\epsilon \geq \epsilon_c$, the system exceeds the stability boundary if the Ruina friction law holds. In the case of the Dieterich law this condition insures that at least quasi-static stick slip should occur (see also sections 8.4 and 8.6).

8.3. Tidal Normal Stress Fluctuations on Faults: Reservoir Effects

We consider two well-known sources of normal (and shear) stress fluctuations on faults: (1) Earth tides which have a period T_{tides} of 12 hours and involve modulations of the loading stress due to the gravitational interactions between the Earth, the Moon and the Sun. (2) Reservoir effects which results in yearly ($T = 1$ year) fluctuations of the loading stress due to annual water depth changes.

The third requirement for resonant destabilization is that the stress fluctuations be of sufficient amplitude. The peak normal stress in tidal loading is expected to be of the order of $\sigma_1 = 10^3$ Pa. Therefore ϵ, the ratio between the normal stress perturbation σ_1 and the total normal stress σ_0, will be of order $\epsilon = 10^{-5}$ for $\sigma_0 = 100$ MPa, representing overburden minus hydrostatic pore pressure at $\simeq 5$ km depth. Such ϵ could destabilize slip only for k very, very close to k_c. It is possible, however, that much of the background seismicity, and of aftershock sequences, nucleates at locations of anomalously low effective stress; weak regions should fail most readily. Such anomalies are not well constrained but could be due to locally elevated pore pressure or to very low local normal stress associated with geometric irregularities along a fault trace (scenario 3). Nevertheless, these would have to be extreme, reducing σ_0 to 1 MPa, to bring the associated ϵ up to 10^{-3}. Even at $\epsilon = 10^{-3}$, we could expect destabilization, by equation (46), only for fault segments with a stiffness which is ~ 5 % above k_c. The situation is even less likely for reservoir fluctuations which involve smaller fluctuations than the tidal σ_1, at least outside the vicinity near the reservoir.

Recall that for scenarios 2 and 3, the linkage (50) between the mean normal stress σ_0 and the period T of normal stress variations must hold if we are to simultaneously meet the first ($T \simeq T_c$) and second ($h \simeq h_c$) requirements for resonance for representative values of a, $b-a$, and tectonic stressing rates. For tidal loading, $T = 12$ hours $=$ yr/730, leading from (50) to $\sigma_0 = 10^{-4}$ to 10^{-3} MPa. These values are irrelevantly small stress levels and shows that there is no possibility that scenarios 2 and 3 could ever be consistent with tidal resonance. Yearly reservoir fluctuations for which $T = 1$ year require $\sigma_0 = 0.1$ to 1 MPa for resonance. These are still very small stress levels. They might be approached by the effective stress only at very shallow depth (5 to 50 m range) under a reservoir. That is an highly restricted case. For it, we could at least be sure that the ϵ, corresponding to stress changes due to annual water depth changes of a couple meters or so, would be large enough.

So the basic conclusion is that scenarios 2 and 3 would, for all practical purposes, not be consistent with resonant triggering on seismically active fault systems. No uncertainties in choice of L, which canceled out enroute to (50), can change that conclusion and neither can variations of a and $b-a$ over a very wide range.

Scenario 1, when the velocity-weakening fault patch is bordered by creeping material, is, however, a viable candidate for allowing regions of size less than h_c to slip at a speed V_0 compatible with $T = T_c$. That is because, unlike for the last two scenarios, the fault surroundings are not locked but slip at the average creep

rate. Using a and b values like in Table 1, the condition $T_{\text{tide}} = T_c$ requires that the slip rate must be in the range of $V_0 = 0.2 \times 10^{-9}$ m s^{-1} (6 mm yr^{-1}) when $L = 1\,\mu$m, to $V_0 = 2 \times 10^{-9}$ m s^{-1} (60 mm yr^{-1}) when $L = 10\,\mu$m. These values are in the range of plate velocities and surface creep rates. Thus it is plausible that some fraction of velocity strengthening patches on an otherwise creeping fault could be susceptible to resonance, at least if their size is near h_c and if their effective stress σ_0 is quite low (of order 1 MPa or less) so as to make ϵ large enough. However, if the value of L for such natural fault patches is substantially larger than 1 to 10 μm, then from (48) we see that the V_0 required for resonance would be well above the plausible range of creep slippage rates on faults in the Earth, and resonance conditions could not be met. For example, with $L = 1$ mm and other parameters like in Table 1, $V_0 = 2 \times 10^{-7}$ m s^{-1} (6 m yr^{-1}). For annual fluctuations of reservoir levels, using a and b values like in Table 1, and $L = 1$ to $10\,\mu$m, the corresponding range is $V_0 \simeq 10^{-5}$ to 10^{-4} m yr^{-1} to make $T = T_c$.

Assuming that some fault patches in scenario 1 do exist that are susceptible to resonant destabilization, there is the remaining difficulty that we do not have a way of estimating, from our considerations here, when ruptures of those velocity-weakening zones might break out onto velocity-strengthening parts of the fault and cause an earthquake over a region of spatial extent that is considerably larger than the rather meager size expected for h_c.

8.4. "Aseismic" Stick Slip

In Figures 5a and 5b we have seen a change from creep to stick slip due to an increase of the normal stress perturbation ϵ. This transition occurs for very low ϵ (of the order of ϵ_c) when close to resonance. Figure 9 shows the normalized velocity V/V_0 as a function of normalized time t/T_c using the Dieterich or ageing law for the same parameters as in Figure 5a. The velocity shows alternations between periods of locking ($V \simeq 10^{-5}V_0$) to periods of rapid increase (up to $V \simeq 10^5 V_0$), which is characteristic of stick-slip behavior. Unlike the Ruina law, the Dieterich law is stable to all perturbations for stiffness greater than k_c. These "earthquake"-like events are quasi-static ones (i.e., inertia can be neglected in the calculation if V_0 is small enough, similar to the 10^{-9} m s^{-1} used here). The average displacement observed during these events is small and of the order of $20L$. These results suggest, assuming that the Dieterich law applies for real faults, that such earthquakes would be very difficult to detect and may belong to the category of the so-called creep burst. This feature should be confirmed using full continuum elastodynamics modeling. These slow, aseismic stick-slip events have no equivalent in the Ruina law framework where inertia can not be neglected. This again emphasizes the need to probe the differences in predictions of these two laws.

8.5. Nucleating Earthquakes

In general, it is expected that when earthquakes nucleate in a modestly nonuniform stress field, increasing

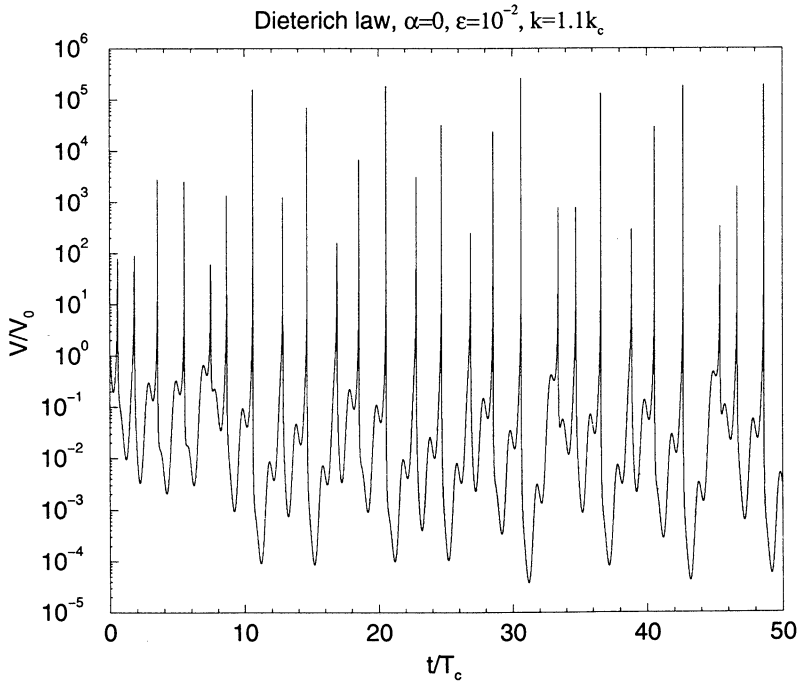

Figure 9. Normalized velocity V/V_0 as a function of normalized time t/T_c using the Dieterich or ageing law for $\alpha = 0$, $k = 1.1k_c$, and $T = T_c$. The rest of the parameters are given in Table 1. The related shear strength is given in Figure 5a. The velocity shows alternations between periods of locking ($V \simeq 10^{-5}V_0$) to periods of rapid increase (up to $V \simeq 10^5 V_0$), which is characteristic of stick-slip behavior. These events occur quasi-statically, that is inertia is negligible for the low V_0 used.

slowly in time on a fault of uniform velocity-weakening properties, aseismic slip (at rates above some exponentially small level corresponding to "locking") will begin in the place of highest stress. The aseismically slipping zone then slowly grows in size until it reaches a size that is comparable to h_c, or at least a size that scales with h_c but may be a few times it [*Lapusta et al.*, 2000]. At that point, there is a rapid break-out into a seismically propagating rupture. Several calculated examples of nucleation phases, dynamic ruptures and the transitions between these two modes of deformation are given, for example, by *Rice and Ben-Zion* [1996], *Ben-Zion and Rice* [1997] and *Lapusta et al.* [2000]. This creeping area may be significant in size when the product $\sigma_0(b-a)$ is very low due for example to high pore pressure.

Our results were obtained in the stable regime assuming that the equivalent stiffness ($K_{eq}(\xi)$) of the sliding surface and the driving velocity do not vary with time. They may be extended to slowly growing patches of dimension less than the nucleation size h_c (so that K_{eq} is greater than the critical stiffness k_c) if their rate of growth is much smaller than the period of the normal stress variations and if they spend sufficiently long time (compared to T) at the range of V which matches T to T_c. That range of V is, from (48), 6 to 60 mm yr^{-1} for $L = 1$ to $10\,\mu$m and for a and b as in Table 1, and certainly, fault segments pass through such a velocity range on their way to instability. However, the issue is whether their residence time in that range is long enough relative to T for resonance to take place (assuming also that σ_0 is low enough to make $\epsilon > \epsilon_c$).

It is not clear if nucleating patches preceding the earthquake instability verify that condition. *Dieterich* [1992] found, using a plane strain fault model with rate-and-state friction laws, that the duration of the nucleation phase can be as long as the interseismic time if the initial stress is close to its steady state value. Nevertheless, V can change appreciably over slips of order L during what ultimately becomes a self-driven creep process leading to instability.

The analysis based on the SB model does not provide a suitable way of evaluating normal stress perturbations on a patch in the late stage of nucleation ($h \simeq h_c$), when growth of the region cannot be neglected. That must be studied using a continuum elastostatic or, better, elastodynamic framework and is left for future work. It may also be important to dynamic triggering of one earthquake by another due to seismic stress oscillations

8.6. Earthquake on Creeping Faults

The generation of small earthquakes on creeping faults is generally interpreted as arising from the existence of unstable patches which are of small size (but nevertheless of a size greater than h_c, so that events can nucleate within them), surrounded by larger stable regions that creep [see *Rubin et al.*, 1999]. Our considerations, subject to the major caveats for scenario 1 resonance in section 8.3, give an alternative explanation, which might be kept in mind. In it, the presence of velocity-weakening regions whose size is large enough to make them unstable is not required, although they would have to closely approach such size.

9. Discussion and Conclusion

In the stable domain ($k > k_c$) we found a resonance phenomenon when a temporally periodic perturbation (of period T) of the normal stress is applied. This resonance depends on the stiffness k as well as on the Linker-Dieterich α parameter.

As can be expected, in Appendix B we show that a resonance is also found for periodic variations of the loading shear stress. This phenomenon is quite different from the resonance in normal stress when one looks in details at the influence of the parameter α or stiffness k, but analytical derivations given in Appendix B show that close to critical stiffness, the resonance occurs for $T = T_c$, the response of the system being unbounded to a first-order approximation. The change from creep to stick-slip behavior is also observed for high enough amplitudes (of the order of ϵ_c). Therefore most of the results obtained in this paper on the stability of the sliding regime (namely, transition from creep to stick slip) can be extended to the case of periodic perturbations of the shear stress and more generally to any type of periodic fluctuations of the external loading acting on a creeping surface.

The sensitivity to normal stress α has been derived from friction experiments [see *Linker and Dieterich*, 1992; *Richardson and Marone*, 1999] on rocks at variable normal stress. Rock friction always implies the existence of a gouge, and it is not clear if this parameter comes from the presence of this gouge or is a general feature of any friction experiment conducted at variable normal stress. Indeed, the *Prakash* [1998] results on friction of metals against a cutting tool material at variable normal stress differ significantly from the ones mentioned above. This discrepancy is not yet explained, even though we can reconcile the two points of view if we consider that α is equal to the coefficient of friction μ. However, *Linker and Dieterich* [1992] and *Richardson and Marone* [1999] found values of α that are different from the steady state coefficient of friction so setting α to μ would only be acceptable at timescales much shorter than the ones accessible to *Linker and Dieterich* [1992] and *Richardson and Marone* [1999], e.g., possibly during unstable dynamic slip. When the parameter α is equal to 0, a resonance peak in shear stress is always observed, while for α different from 0 this resonance disappears for a large enough stiffness. This is an illustration of the stabilizing effect of the α parameter. This feature is also illustrated by the fact that the higher α, the lower the maximal stress drop of the system. However, this stabilizing effect is limited since α can only vary from 0 to μ, where μ is the coefficient of friction.

The Dieterich and Ruina laws both roughly fit the data inferred from laboratory friction experiments on rocks. When using the Ruina law, slip is necessary for friction to evolve, while for the Dieterich law, friction can evolve without displacement (growth of the static ($V = 0$) coefficient of friction with time). Both laws have shortcomings, as discussed by *Beeler et al.* [1994] and *Marone* [1998]. The Dieterich law seems to be more suitable to the description of frictional behavior during slide-hold-slide tests, whereas the Ruina law is favored in representing behavior around steady state. To our knowledge, neither of them could be preferred as long as the normal stress is constant. However, *Richardson and Marone* [1999] showed that the Ruina law seems to fit the data at variable normal stress better than the Dieterich one which, for instance, overshoots the final steady state shear stress in normal stress step experiments. They also show different response to finite perturbations, since the Ruina law is conditionally stable for a stiffness greater than the critical stiffness k_c while the Dieterich one is not. This difference is also observed when finite normal stress perturbations are considered (see section 3). The transition from creep to stick-slip behavior results in the generation of quasi-static aperiodic events when the ageing law is considered, while for the case of the slip law the observed sequence of events is periodic (as long as α is different from μ_{ss}) and inertia has to be considered (due to the crossing of the stability boundary).

Possible applications of our results to laboratory experiments exist. First, we have to estimate the magnitude of the resonance periods. The resonance period T_r is of order $T_c = 2\pi\sqrt{a/(b-a)}L/V_0$. Since b is sometimes of order $2a$ in friction experiments on rocks, we can roughly write that T_c is of order $2\pi L/V_0$. The characteristic length of evolution of friction L is usually of order $10\,\mu$m on rough surfaces. Using a loading speed V_0 of order $10\,\mu\text{m s}^{-1}$ would then give a period of resonance of the order of 1 s (i.e., a frequency of 1 Hz) and should be observable in laboratory experiments. For choosing between these two friction laws we also suggest applying an oscillating perturbation in the normal stress close to the stability boundary ($k = k_c + \delta k$, with $\delta k > 0$ and $\delta k \ll k_c$) and then adjusting the period of the oscillation to the resonance period. Equivalently, for a given stiffness the normal stress may be set slightly below its critical value. Once at resonance, the perturbation ϵ should be slowly raised from very small (10^{-4}) to large (10^{-2}) (see section 5 and Figures 5a and 5b). Figures 5a and 5b illustrate the potential experimental difficulty to discriminate one law from the other since they both show stick slip events. A study of the stress drop evolution with respect to the perturbation amplitude ϵ might provide a useful tool in this case (as shown in Figure 4). A discontinuous stress drop evolution as stick slip appears will be consistent with the Ruina law. We emphasize that one should not expect either one of these two laws to fully apply. What we propose are new type of experiments which may help experimentalists to obtain the appropriate framework to describe the evolution of friction at variable normal stress.

Preliminary estimates made here raise doubts that the resonance phenomena could contribute to tidal interactions with earthquakes, except in the case when the events nucleate on velocity-weakening fault patches that are small enough to be stiffness-stabilized, and which reside within velocity-strengthening fault planes that are creeping (scenario 1), as suggested by *Boatwright and Cocco* [1996]. For some subset of such zones the creep rate could be matched to the rate (~ 6 to 60 mm yr^{-1}) required for resonant driving. Then, if the effective normal stress was exceptionally low, we think as low as 1 MPa, the amplitude of tidal stressing could be large enough to cause the resonant destabilization on, say, those stiffness-stabilized fault patches which are within $\sim 5\%$ of critical size. There remains the issue that the subsequent earthquake rupture area would be small unless the velocity-strengthening outside those patches was very weak [*Boatwright and Cocco*, 1996].

Direct triggering due to earth tides has been studied by *Vidale et al.* [1998] by looking at the possible correlations between the rate of earthquake production at peak tidal stress and stress rate. A correlation is observed but is too small to be statistically significant. We suspect that tidal triggering of earthquakes on creeping faults, if not necessarily the resonance phenomenon discussed here, may exist even though its detection seems to be a complex problem, the response of the fault being highly nonlinear. As shown by *Gomberg et al.* [1998] using a SB model, the advance (or delay) in failure time of earthquakes due to static and transient changes of the shear stress highly depends on the initial state of stress and is not constant as in the classic Coulomb friction (constant μ). Ongoing studies [*Perfettini and Schmittbuhl*, 2001] focus on the implications of our analysis on tidal triggering of earthquakes including description of the measurement biases resulting from phase lag scattering on fault heterogeneities.

Appendix A: Evolution of Friction Due to an Instantaneous Step in Normal Stress

When a fault undergoes a change in conditions, the change in shear stress is

$$d\tau = \sigma d\mu + \mu d\sigma. \tag{A1}$$

When the fault is sliding at constant V,

$$d\mu|_{V=\text{const}} = d\mu(V,\psi)|_{V=\text{const}} = d\psi. \tag{A2}$$

Also, when there is an instantaneous ($dt \to 0$) step change in normal stress,

$$d\psi|_{dt\to 0} = -\alpha d\sigma/\sigma. \tag{A3}$$

Combining (A2) and (A3), for an instantaneous step $d\sigma$ while the slip rate is maintained constant,

$$d\mu|_{V=\text{const},\, dt\to 0} = -\alpha d\sigma/\sigma, \tag{A4}$$

and inserting that into (A1) gives

$$d\tau|_{V=\text{const},\, dt\to 0} = (\mu - \alpha)d\sigma. \tag{A5}$$

So, if $\alpha = \mu(V,\psi)$, there is no instantaneous change in friction following an instantaneous change in normal stress. Integrating (A3) for an instantaneous finite step in normal stress, one gets

$$\psi|_{dt\to 0} = \psi_0 - \alpha \ln(\sigma/\sigma_0), \tag{A6}$$

where ψ_0 and σ_0 are the values of ψ and σ prior to the step in normal stress. It follows that μ is a function of the fixed velocity V and of the normal stress σ during any such instantaneous step (and so will be α if we assume that $\alpha = \mu$)

Appendix B: Case of Periodic Variations in Shear and Normal Loading Stress

When periodic perturbations in an externally applied shear stress loading of the block $\tau_e(t) = \tilde{\tau}\sin(\omega t)$ are considered, (12) transforms to

$$m\frac{dV}{dt} = ku - \tau + \tau_e(t), \tag{B1}$$

so that when $m = 0$ (22) becomes

$$\tau_1 = ku_1 + \tilde{\tau}, \tag{B2}$$

and (20), (21), and (23) remained unchanged. This leads to a change in frictional shear stress τ_1 given by

$$\begin{aligned}\frac{\tau_1}{\sigma_1\mu_{ss}} = {} & [(\sigma_1\mu_{ss} - \tilde{\tau}(\frac{q}{q_c})^2(\frac{k_c}{k})) + \\ & iq(\sigma_1(\mu_{ss}-\alpha) - \tilde{\tau}(\frac{k_c}{k}))]/ \\ & [1 - \frac{a\sigma_0 q^2}{kL} + iq(1-\frac{k_c}{k})],\end{aligned} \tag{B3}$$

and a velocity change V_1

$$V_1/V_0 = (\frac{q}{kL})\frac{q[\sigma_1(\mu_{ss}-\alpha)-\tilde{\tau}] - i[\sigma_1\mu_{ss}-\tilde{\tau}]}{1 - \frac{a\sigma_0 q^2}{kL} + iq[1-\frac{k_c}{k}]}. \tag{B4}$$

The denominator of τ_1 and V_1 still vanishes when $q = q_c$ and $k = k_c$, leading to an unbounded response of the system. As can be verified using (B3) or (B4), the resonance phenomenon is also observed in presence of periodic variations in shear stress and is therefore a general feature of periodic changes in the loading stress.

Acknowledgments. J. R. Rice was supported by a Blaise Pascal Chair for 1999 from the Foundation of Ecole Normale Supérieure and by USGS grant 99-HQ-GR-0025. We are grateful to Y. Ben-Zion, J. Gomberg, and M. Campillo for thoughtful reviews. We would also like to thank R. Madariaga, A. Cochard, J.-P. Ampuero, R. S. Stein, J.-P. Vilotte, and D. Lockner for essential discussions and suggestions.

References

Adams, G. G., Self-excited oscillations of two elastic half-spaces sliding with a constant coefficient of friction, *J. of Appl. Mecha.*, *62*, 867–872, 1995.

Andrews, D. J., and Y. Ben-Zion, Wrinkle-like slip on a fault between different materials, *J. Geophys. Res.*, *102*, 553–571, 1997.

Baumberger, T., C. Caroli, B. Perrin, and O. Ronsin, Nonlinear analysis of the stick-slip bifurcation in the creep-controlled regime of dry friction, *Phys. Rev. E*, *51*, 4005–4010, 1995.

Beeler, N. M., T. E. Tullis, and J. D. Weeks, The roles of time and displacement in the evolution effect in rock friction, *Geophys. Res. Lett.*, *21*, 1987–1990, 1994.

Ben-Zion, Y., and J. R. Rice, Dynamic simulations of slip on a smooth fault in an elastic solid, *J. Geophys. Res.*, *102*, 17,771–17,784, 1997.

Blanpied, M. L., D. A. Lockner, and J. D. Byerlee, Fault stability inferred from granite sliding experiments at hydrothermal conditions, *Geophys. Res. Lett.*, *18*, 609–612, 1991.

Boatwright, J., and M. Cocco, Frictional constraints on crustal faulting, *J. Geophys. Res.*, *101*, 13,895–13,909, 1996.

Burridge, R., and L. Knopoff, Model and theoritical seismicity, *Bull. Seismol. Soc. Am.*, *57*, 341–371, 1967.

Carlson, J. M., and J. S. Langer, Mechanical model of an earthquake, *Phys. Rev. A Gen. Phys.*, *40*, 6470–6484, 1989.

Cochard, A., and R. Madariaga, Dynamic faulting under rate-dependent friction, *Pure Appl. Geophys.*, *142*, 419–445, 1994.

Cochard, A., and R. Madariaga, Complexity of seismicity due to highly rate dependent friction, *J. Geophys. Res.*, *101*, 25,321–25,336, 1996.

Cochard, A., and J. R. Rice, Fault rupture between dissimilar materials: Ill-posedness, regularization, and slip-pulse response, *J. Geophys. Res.*, *105*, 25,891–25,907, 2000.

Dieterich, J. H., Modeling of rock friction, 1, Experimental results and constitutive equations, *J. Geophys. Res.*, *84*, 2161–2168, 1979a.

Dieterich, J. H., Modeling of rock friction, 2, Simulation of presesimic slip, *J. Geophys. Res.*, *84*, 2169–2175, 1979b.

Dieterich, J. H., Constitutive properties of faults with simulated gouge, in *Mechanical Behavior of Crustal Rocks, Geophys. Monogr. Serv.*, edited by N. L. Carter, M. Friedman, J. M. Logan, and D. W. Stearns, vol. 24, pp. 103–120. AGU, Washington, D.C., 1981.

Dieterich, J. H., Earthquake nucleation on faults with rate- and state-dependent strength, *Tectonophysics*, *211*, 115–134, 1992.

Dieterich, J. H., and M. F. Linker, Fault stability under conditions of variable normal stress, *J. Geophys. Res.*, *97*, 4923–4940, 1992.

Gomberg, J., N. M. Beeler, M. L. Blanpied, and P. Bodin, Earthquake triggering by transient and static deformations, *J. Geophys. Res.*, *103*, 24,411–24,426, 1998.

Gu, J., J. R. Rice, A. L. Ruina, and S. T. Tse, Slip motion and stability of a single degree of freedom elastic system with rate and state dependent friction, *J. Mech. Phys. Solids*, *32*, 167–196, 1984.

Guatteri, M. G., and P. Spudich, What can strong-data tell us about slip-weakening fault friction laws?, *Bull. Seismol. Soc. Am.*, *90*, 98–116, 2000.

He, C., S. Ma, and J. Huang, Transition between stable sliding and stick-slip due to variation in slip rate under variable normal stress condition, *Geophys. Res. Lett.*, *25*, 3235–3238, 1998.

Heslot, F., T. Baumberger, B. Perrin, B. Caroli, and C. Caroli, Creep, stick-slip, and dry-friction dynamics: Experiments and a heuristic model, *Phys. Rev. E*, *49*, 4973–4988, 1994.

Horowitz, F. G., and A. Ruina, Slip patterns in a spatially homogeneous fault model, *J. Geophys. Res.*, *94*, 10.279–10.298, 1989.

Lapusta, N., J. R. Rice, Y. Ben-Zion, and G. Zheng, Elastodynamic analysis for slow tectonic loading with spontaneous rupture episodes on faults with rate- and state-dependent friction, *J. Geophys. Res.*, *105*, 23,765–23,789, 2000.

Linker, M. F., and J. H. Dieterich, Effects of variable normal stress on rock friction: Observations and constitutive equations, *J. Geophys. Res.*, *97*, 4923–4940, 1992.

Madariaga, R., and A. Cochard, Seimic source dynamics, heterogeneity and friction, *Ann. Geofisi.*, *37*, 1349–1375, 1994.

Marone, C. J., Laboratory-derived friction laws and their application to seismic faulting, *Annu. Rev. Earth Planet. Sci.*, *26*, 643–696, 1998.

Marone, C. J., and B. Kilgore, Scaling of the critical slip distance for seismic faulting with shear strain in fault zones, *Nature*, *362*, 618–621, 1993.

Marone, C. J., C. H. Scholz, and R. Bilham, On the mechanics of earthquake afterslip, *J. Geophys. Res.*, *96*, 8441–8452, 1991.

Martins, J. A. C., and F. M. F. Simões, On some sources of instability/ill-posedness in elasticity, in *Contact Mechanics*, edited by M. Raous, M. Jean, and J. J. Moreau, pp. 95–106. Plenum, New York, 1995.

Okubo, P., Dynamic rupture modeling with laboratory-derived constitutive relations, *J. Geophys. Res.*, *94*, 12,321–12,335, 1989.

Parsons, T., R. S. Stein, R. W. Simpson, and P. A. Reasenberg, Stress sensivity of fault seismicity: A comparison between limited-offset thrust and major strike-slip faults, *J. Geophys. Res.*, *104*, 20,183–20,202, 1999.

Perfettini, H., and J. Schmittbuhl, Periodic loading on a creeping fault: Implications for tides, *Geophys. Res. Lett.*, *28*, 435–438, 2001.

Perfettini, H., R. S. Stein, R. W. Simpson, and M. Cocco, Stress transfer by the 1988-1989 M=5.3, 5.4 Lake Elsman foreshocks to the Loma Prieta fault: Unclamping at the site of peak mainshock slip, *J. Geophys. Res.*, *104*, 20,169–20,182, 1999.

Prakash, V., Frictional response of sliding interfaces subjected to time varying normal pressures, *J. Tribol.*, *120*, 97–102, 1998.

Prakash, V., and R. J. Clifton, Time resolved dynamic friction measurements in pressure-shear, in *Expererimental Techniques in the Dynamics of Deformable Solids*, vol. AMD-165, pp. 33–48. Appl. Mech. Div., ASME, New York, 1993.

Press, W. H., B. P. Flannery, S. A. Teukolsky, and W. T. Vetterling, Integration of ordinary differential equations, in *Numerical Recipes in C, The Art of Scientific Computing, 2nd ed.*, pp. 707–752. Cambridge Univ. Press, New York, 1992.

Ranjith, K., and J. R. Rice, Stability of quasi-static slip in a single degree of freedom elastic system with rate and state dependent friction, *J. Mech. Phys. Solids*, *47*, 1207–1218, 1999.

Rice, J. R., Spatio-temporal complexity of slip on a fault, *J. Geophys. Res.*, *98*, 9885–9907, 1993.

Rice, J. R., and Y. Ben-Zion, Slip complexity in earthquakes models, *Proc. Natl. Acad. Sci. U.S.A.*, *93*, 3811–3818, 1996.

Rice, J. R., and A. L. Ruina, Stability of steady frictional slipping, *J. of Appl. Mecha.*, *50*, 343–349, 1983.

Rice, J. R., and S. T. Tse, Dynamic motion of a single degree of freedom system following a rate and state dependent friction law, *J. Geophys. Res.*, *91*, 521–530, 1986.

Richardson, E., and C. J. Marone, Effects of normal force vibrations on frictional healing, *J. Geophys. Res.*, *104*, 28,859–28,878, 1999.

Rubin, A. M., D. Gillard, and J.-L. Got, Microseismic lineations along creeping faults, *Nature*, *400*, 635–641, 1999.

Ruina, A. L., Slip instability and state variable fricton laws, *J. Geophys. Res.*, *88*, 10,359–10,370, 1983.

Schmittbuhl, J., J. P. Vilotte, and S. Roux, A dissipation based analysis of an earthquake fault model, *J. Geophys. Res.*, *101*, 27,741–27,764, 1996.

Segall, P., and J. R. Rice, Dilatancy, compaction, and slip instability of a fluid infiltrated fault, *J. Geophys. Res.*, *100*, 22,155–22,171, 1995.

Vidale, J. E., D. C. Agnew, M. J. S. Johnston, and D. H. Oppenheimer, Absence of earthquake correlation with Earth tides: An indication of high preseimic fault stress rate, *J. Geophys. Res.*, *103*, 24,567–24,572, 1998.

Weertman, J. J., Unstable slippage across a fault that separates elastic media of different elastic constants, *J. Geophys. Res.*, *85*, 1455–1461, 1980.

M. Cocco, Istituto Nazionale di Geofisica, Via di Vigna Murata 605, 00143 Rome, Italy. (cocco@ing750.ingrm.it)

H. Perfettini, Laboratoire de Géophysique Interne et Tectonophysique, Université Joseph Fourier, BP 53, 38041 Grenoble Cedex 9, France (Hugo.Perfettini@obs.ujf-grenoble.fr)

J. R. Rice, Department of Earth and Planetary Sciences and Division of Engineering and Applied Sciences, Harvard University, 224 Pierce Hall, 29 Oxford Street, Cambridge, MA 02138. (rice@esag.harvard.edu)

J. Schmittbuhl, Laboratoire de Géologie, Ecole Normale Supérieure, 75231 Paris Cedex 05, France. (schmittb@geologie.ens.fr)

(Received December 16, 1999; revised July 28, 2000; accepted October 4, 2000.)